Food Chemistry: X 25 (2025) 102182

Contents lists available at ScienceDirect

Food Chemistry: X

journal homepage: www.sciencedirect.com/journal/food-chemistry-x

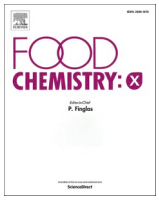

Resveratrol-derived carbon dots integrated into gelatin/chitosan multifunctional films for intelligent packaging

Tianxin Fu [a], Yuchao Feng [c], Shu Zhang [a], Yanan Sheng [a], Changyuan Wang [a,b,*]

[a] College of Food Science, Heilongjiang Bayi Agricultural University, Xinfeng Lu 5, Daqing 163319,China
[b] Chinese National Engineering Research, Daqing 163319,China
[c] Institute of Quality Standards and Testing Technology for Agro-Products of Chinese Academy of Agricultural Sciences, Beijing 100081, China

ARTICLE INFO

Keywords:
Multifunctional carbon dots
Gelatin
Chitosan
Intelligent packaging
Pork

ABSTRACT

In this study, multifunctional Resveratrol-derived carbon dots (Res-CDs) were prepared using a hydrothermal method. Res-CDs exhibited good free-radical scavenging activities, attributed to abundant surface hydroxyl groups, and effectively inhibited *Staphylococcus aureus* and *Escherichia coli* growth at a concentration of 2 mg/mL. Composite films were prepared by combining Res-CDs with gelatin/chitosan. As well as excellent mechanical properties, the prepared films exhibited smooth surfaces, thermal stability, and good antioxidant, ultraviolet-shielding, antibacterial, and pH-responsive properties. Furthermore, cell viability measurements showed that the films were safe. When applied to keeping pork fresh, the gelatin/chitosan/Res-CDs film significantly reduced the total viable bacterial count on the pork surface and effectively prevented pork discoloration. Additionally, pH, total volatile basic nitrogen, and weight loss measurements confirmed the preservative effects of the film on pork. This work provides a new approach for synthesizing bionanocomposite films with applicability in the food industry.

1. Introduction

Food spoilage can have potentially grave health implications, thereby posing a significant threat to food safety while also wasting substantial resources. Plastic packaging materials are recalcitrant to degradation and give rise to severe environmental pollution, thereby posing a grave threat to the survival and ecological balance of human beings, animals, and plants (Calva-Estrada et al., 2019). At the same time, the raw materials utilized for the production of synthetic polymers, such as oil and natural gas are dwindling, and this resource crisis demands an urgent solution.

To address this pressing challenge, the development of novel, multifunctional, and eco-friendly food packaging has emerged as a critical priority. In recent years, to extend products shelf life and ensure food freshness and safety, the food industry has widely adopted advanced packaging strategies, including modified atmosphere packaging (Jia et al., 2019), active packaging (Yildirim et al., 2018), and intelligent packaging (Rekha et al., 2021; Wang, Li, & Hu, 2023). Active food packaging, which involves the incorporation of functional active substances such as antioxidants and antimicrobial agents into films, is aimed at preventing food contamination by microorganisms and effectively suppressing undesirable biochemical changes, thereby maintaining long-term freshness and nutritional value (Settier-Ramirez et al., 2022). In intelligent packaging, embedded sensors and detection mechanisms precisely perceive, detect, and record subtle changes within and around foodstuffs (Fang et al., 2017). These changes trigger adaptive alterations in the packaging to provide consumers intuitive and timely information about food freshness, thus, developing food packaging with both intelligent and active functions is an effective strategy to solve the problems of food safety and waste.

The preparation of biodegradable and edible new packaging materials using natural biodegradable substances has the advantages of easy access to materials, environmental friendliness, and diverse functions (Mohammadi et al., 2018; Uranga et al., 2019). Gelatin has excellent film-forming properties, outstanding safety, and moisture resistance. However, gelatin does not exhibit antibacterial, antioxidant, or ultraviolet (UV)-shielding properties (Chen et al., 2024). Chitosan (CS) has received widespread attention owing to its outstanding antimicrobial activity, nontoxicity, biodegradability, and biocompatibility (Ren et al., 2017). The complementary properties of gelatin and CS can be combined to produce films with significantly improved overall performance. Nevertheless, the antimicrobial and antioxidant activities of unmodified

* Corresponding author at: College of Food Science, Heilongjiang Bayi Agricultural University, Xinfeng Lu 5, Daqing 163319,China.
E-mail address: byndwcy@163.com (C. Wang).

https://doi.org/10.1016/j.fochx.2025.102182
Received 8 November 2024; Received in revised form 22 December 2024; Accepted 12 January 2025
Available online 13 January 2025

gelatin/CS films remain limited and cannot meet the requirements of long-term food preservation (Fu et al., 2022). Therefore, new multifunctional, and safe food preservation materials must be developed.

As an innovative carbon nanomaterial with a size smaller than 10 nm, carbon dots (CDs) have demonstrated extensive application potential in fields such as chemical/biological sensing, biological imaging, and nanomedicine owing to their antioxidant and antibacterial properties, nontoxicity, excellent biocompatibility, UV-shielding ability, and simple synthesis process (Kurian & Paul, 2021). Recently, CDs been found that can provide protection against both UV and blue light (Tripathi et al., 2024), notably, it can be used as pH sensors (Bogireddy et al., 2020). Therefore, CDs are an ideal additive for fabricating multifunctional biocomposite films.

Resveratrol (Res), an endogenous non-flavonoid polyphenol commonly found in traditional Chinese medicine and plant-based foods, has attracted considerable attention owing to medical value, including anti-inflammatory, antioxidant (Liu et al., 2020), anticancer (Oh & Shahidi, 2017), and angiogenesis-promoting properties (Md Shimul et al., 2024). However, the widespread use of Res in practical applications has been limited by its low water solubility, poor absorption, limited bioavailability, and easy decomposition (Li et al., 2019). Thus, to improve the bioavailability of Res, it is necessary to adopt strategies that enhance its water solubility and stability.

The modification of gelatin/CS films with CDs could provide enhanced multifunctional properties suitable for food packaging applications. In this study, we prepared Res-derived CDs (Res-CDs) using a hydrothermal method with Res and citric acid (CA) as precursors and explored their unique structural and fluorescent properties. Res-CDs were then added to a mixture of gelatin and CS to construct a functional bionanocomposite film. The performance of this film was comprehensively evaluated based on the mechanical strength, antioxidant activity, antimicrobial capabilities, pH responsiveness, morphological characteristics, water vapor permeability (WVP), and water contact angle (WCA). Furthermore, quality changes were compared during the preservation of fresh pork with gelatin/CS film, gelatin/CS/Res-CDs film, and untreated groups. Notably, the gelatin/CS/Res-CDs film exhibited excellent performance in maintaining pork quality, with its pH sensitivity being particularly effective for monitoring freshness. Overall, this composite film exhibited potential for use as a smart packaging system.

2. Experimental section

2.1. Materials

Gelatin (240 Bloom), glycerin, Res hydrochloric acid, CS (deacetylation degree: 75–85 %, viscosity: 200–800 P), and acetic acid were purchased from Macklin (Shanghai, China). CA, phosphoric acid, and sodium hydroxide were provided by Guangdong Guanghua Science and Technology Co., Ltd. (Guangdong, China). Penicillin–streptomycin, trypsin–ethylenediaminetetraacetic acid and fetal bovine serum were obtained from Macklin Co., Ltd. (Beiling, China). 2,2′-Azino-bis(3-ethylbenzothiazoline-6-sulfonic acid) (ABTS) and 2,2-diphenyl-1-picrylhydrazyl (DPPH) were supplied by Sigma-Aldrich (Shanghai, China).

2.2. Preparation of res-CDs

Res-CDs were synthesized according to a previously described method with some adjustments (Cheng et al., 2023). Briefly, 0.5 g of Res and 1.0 g of CA were sonicated in deionized water at 100 °C for 30 min, and the mixture was heated in a Teflon-lined stainless steel reactor at 200 °C for 8 h. The precipitate was removed by centrifugation, and the supernatant was collected in a 5000 Da dialysis bag and lyophilized after 2 days of dialysis.

2.3. Characterization of res-CDs

The microstructure of Res-CDs was examined using Transmission Electron Microscopy (TEM; JEOL F200, Japan Electronics Corporation Ltd., Tokyo, Japan). The absorption spectra were obtained using an ultraviolet–visible (UV–Vis) spectrophotometer (60 UV, Shimadzu Ltd., Tokyo, Japan). The surface structure and elemental composition of Res-CDs were investigated via Fourier transform infrared (FTIR) spectroscopy and X-ray photoelectron spectroscopy (XPS). FTIR spectra were gathered within the range of 500–4000 cm^{-1} using a Nicolet 8700 spectrometer (Thermo Scientific, Waltham, MA, USA), while XPS spectra were obtained with an Escalab 250Xi spectrometer (Thermo Scientific, USA). The fluorescence (FL) emission spectra of Res-CDs within the excitation wavelengths of 310–380 nm was recorded using a FL spectrophotometer (F6200, Shanghai Ling guang Technology Co., Ltd., China). For pH sensing, the FL intensity was determined at the optimal excitation wavelength for pH values of 4.0, 5.0, 6.0, 7.0, and 8.0, and the fluorescence emission spectra were obtained in the range of 300 nm to 600 nm.

2.4. Functional properties of res-CDs

2.4.1. Antioxidant properties of res-CDs

The antioxidant properties of Res-CDs were measured through DPPH and ABTS radical scavenging assays. For these measurements, 100 μL of Res-CDs solution was mixed with 3.9 mL of DPPH or ABTS solution. The absorbance of the mixture was measured at 515 or 734 nm, respectively, in a dark environment. Solutions without Res-CDs were used as controls (Chen et al., 2020). DPPH and ABTS scavenging rates were calculated using the following Eq. (1):

$$(A_1 - A_2)/A_1 \times 100\% \quad (1)$$

where A_1 and A_2 represent the the absorbance values at 515 nm/734 nm for the control and Res-CDs samples, respectively, at each concentration.

2.4.2. Antimicrobial properties of res-CDs

The antimicrobial activity of Res-CDs was evaluated following a modified previously described method (Guo et al., 2024). *Staphylococcus aureus* and *Escherichia coli* were cultured in Luria broth at 37 °C for 12 h. The optical density (OD) of the bacteria at 600 nm was used to represent the bacterial concentration. The bacterial suspension was diluted with the liquid medium to obtain an OD of 0.1 at 600 nm and then further diluted 100 times. 100 μL of the bacterial suspension was added to a 96-well plate. Subsequently, 100 μL of bacterial suspension and 100 μL of Res-CDs solution (concentrations of 0.5, 1.0, 1.5, and 2 mg/mL) were added to a 96 well plate and co-cultured at 37 °C for 24 h. The OD of the sample was determined every 3 h to confirm bacterial growth curves. Then, 20 μL of the Res-CDs and bacteria mixture was applied to an agar plate and incubated for 24 h at 37 °C. The bacterial viability was calculated using Eq. (2).

$$OD600_{-1}/OD600_{-2} \times 100\% \quad (2)$$

where $OD600_{-1}$ refers to the OD at 600 nm after co-incubation of Res-CDs with bacteria for 24 h and $OD600_{-2}$ is the OD at 600 nm of the bacterial solution grown without Res-CDs for 24 h.

2.5. Cytotoxicity of res-CDs

Caco-2 cells were cultured in 5 % CO_2 medium at 37 °C for 24 h, roughly 8000 cells were transplanted into 96-well plates. Subsequently, the cells were treated with Res-CDs at concentrations of 0, 50, 100, 200 and 400 μg/mL for 24 h. Subsequently, the medium was removed and the cells were washed with phosphate-buffered saline (pH 7.2) before adding 100 μL of 0.5 mg/mL MTT, and incubated for 4 h. After removing the solution, 100 μL of dimethyl sulfoxide was added to each well. The

absorbance was measured at 490 nm after 10 min of gentle shaking to calculate the cell viability as follows:

$$\text{Cell viability}\ (\%) = (A_s - A_b)/(A_c - A_b) \times 100 \quad (3)$$

where A_s, A_c, and A_b are the absorbance values of the sample, control, and background, respectively.

2.6. Film preparation

The film was prepared based on a modification of a previously reported method (Haghighi et al., 2019). Specifically, 10 g of gelatin dissolved in 200 mL of deionized water and stirred at 50 °C for 1 h. In addition, 5 g of CS was mixed with 1 % acetic acid solution (100 mL) and stirred continuously for 1 h at 80 °C. Then, 200 mL of the gelatin solution was mixed with 100 mL of the CS solution and 0.5 %, 1 %, 1.5 %, or 2 % (m/v) of Res-CDs was added, respectively. After vigorously stirring for 2 h at 50 °C, 1 % (m/v) glycerol was added as a plasticizer. The films were obtained by pouring the mixed solution onto a glass plate and dried.

2.7. Film properties

2.7.1. Mechanical properties

The intelligent electronic tensile tester (Jinan Zhongce Electromechanical Equipment Co., Ltd) was used to measure the tensile strength (TS) and elongation at break (EB) of films. A strip of film (10 cm × 2.5 cm) was fixed to the machine for tensile testing. The initial grip length was set to 60 mm and the crosshead speed to 25 mm/min. Each sample was analyzed five times.

2.7.2. WVP and WCA

The WVP of the thin films was measured according to Ezati (Ezati et al., 2023). The surface wettability of the films was evaluated using the WCA, as measured using a contact angle analyzer (CA100, Guangdong Hokuto Instrument Co., Ltd., Guangdong, China) according to the procedure of Ezati (Ezati et al., 2023).

2.7.3. Antioxidant properties

The antioxidant capacities of the thin films were determined by a previously reported method (Sul et al., 2023). Add a 50 mg piece of film to 10 mL of a DPPH or ABTS solution with an absorbance value of 0.7 ± 0.02. The absorbance was measured at 515 or 734 nm after reacting in the dark for 30 min. The DPPH and ABTS scavenging activity were using Eq. (1).

2.7.4. Antimicrobial capacities

Evaluation of the antimicrobial capacity of the film by measuring the reduction in the number of colonies after direct contact with the film (Min et al., 2022). Briefly, *S. aureus* or *E. coli* was activated by cultivation in liquid medium (Luria-Bertani) at 37 °C for 24 h. The OD of the bacterial suspension was adjusted to 0.1 at 600 nm and then diluted 100 times. Then, 1 mL of bacterial solution was added to a 6-well plate containing films with Res-CDs contents of 0 %, 0.5 %, 1 %, 1.5 %, or 2 % and the mixture was cocultured for 2 h at 37 °C. Then, 20uL of bacterial suspension was uniformly coated on the solid culture medium and incubated at 37 °C for 48 h. The antibacterial activity(%) was calculated according to Eq. (3).

$$\text{Antibacterial rate}\ (\%) = (1 - N_1/N_2) \times 100\% \quad (4)$$

where N_1 and N_2 are the number of bacterial colonies in the film-treated and control groups, respectively.

2.7.5. Optical properties

Composite film containing 1.5 % Res-CDs was immersed in BR buffer solutions with pH values of 5.5, 6.0, 6.5, 7.0, and 7.5, respectively. Subsequently, the FL emission spectra were recorded at 340 nm, with the range of 300–600 nm. In addition, to ensure the fluorescence stability of gelatin/chitosan/Res-CDs films in natural environments, they were exposed to natural environments for 1–9 days and the fluorescence intensity of the films was measured. The UV–Vis absorption spectra of the films containing 0, 0.5, 1.5 and 2.0 % Res-CDs were obtained in the range of 200 nm to 800 nm via a UV–Vis spectrophotometer (Specord 50 plus, JENA, Germany).

2.8. Morphology and structure

The surface morphology of the composite films were observed via scanning electron microscopy (SEM). The surface structures and roughnesses of the films were investigated through atomic force microscopy (AFM; SPM-9700, Dimension Icon, Japan). In addition, the FTIR spectra of the films were recorded using 32 scans within 500–4000 cm^{-1}.

2.9. Cytotoxicity

According to a previously reported approach, the cytotoxicity of the films was measured adopting the MTT method (Liu et al., 2024). Initially, the composite membranes were disinfected using UV radiation for 30 min. A 15 mg piece of the thin film was immersed in 2 mL of the liquid culture medium for a period of 24 h. The medium was then filtered through a 0.22 μm membrane and the filtrate was collected and set aside (experimental group). After Caco-2 cells were cultured in 5 % CO_2 medium at 37 °C for 24 h, roughly 8000 cells were transplanted into 96-well plates. Then, either 100 μL of liquid medium (control group) or 100 μL of filtrate (experimental group) was added into the 96-well plates and incubated for 24 h. Subsequently, the medium was removed and the cells were washed with phosphate-buffered saline (pH 7.2) before adding 100 μL of 0.5 mg/mL MTT, and incubated for 4 h. Follow up experimental steps refer to 2.5.

2.10. Packaging test

The packaging properties of the gelatin/CS/Res-CDs film containing 1.5 % Res-CDs were investigated using a packaging test with pork tenderloin procured from a local Wanhui supermarket. Pork of evenly colored was selected, cut into cuboids of evenly size, and wrapped in the gelatin/CS or gelatin/CS/Res-CDs film. The pH, total volatile basic nitrogen (TVB-N), total viable bacteria count (TVC), thiobarbituric acid (TBA) and pork weight were measured on day 0, day 1, day 2, day 3, day 4, day 5, and day 6. The pH, TVB-N, TBA and TVC values were determined using the methods outlined in the National Standard of the People's Republic of China (GB/T 9695.5–2008, GB 5009.228–2016, GB 5009.18–2016 and GB 4789.2–2016, respectively). In addition, the FL emission spectra of the composite film were recorded on the corresponding day. The specific experimental method is described in 2.6.5. The color value of the pork samples were accessed with a colorimeter (CR-410; Konica Minolta, Tokyo, Japan).

3. Results and discussion

3.1. Characterizations of res-CDs

A one-step hydrothermal method with Res and CA as precursors produced well-dispersed, non-aggregated, and highly stable Res-CDs. The Fig. S1a illustrated that Res-CDs were mostly spherical and uniformly sized, with an average size of 6.87 nm. High resolution transmission electron microscopy examination shows that these particles had a unique lattice structure with a interplanar spacing of 0.21 nm, corresponding to the {100} crystal plane of graphene. The FTIR spectrogram (Fig. S1b) shows that the peaks of Res-CDs at 3349 cm^{-1}, 1650 cm^{-1} and 1506 cm^{-1} were due to the vibrations of O—H, C═O and C═C bonds in

the aromatic ring, respectively (Riahi et al., 2022). The peak at 1320 cm^{-1} was attributed to the vibrations of carboxyl groups (–COOH), and those at 1150 and 1049 cm^{-1} corresponded to stretching vibrations of C—O bonds (Zhao, Zhang, et al., 2022). These results indicated that CA condensed with Res and then further carbonizes to form graphite carbon nuclei with hydrophilic functional groups such as -OH and -COOH on the surface.

The XPS results revealed that Res-CDs were predominantly of carbon (72.69 %) and oxygen (28.31 %) elements (Fig. S1c). The high-resolution C 1 s spectrum (Fig. S1d) shows that the characteristic peaks of Res-CDs at 283.6, 285.9, and 289.2 eV corresponded to the C-C/C=C, C—O, and C═O functional groups, respectively, confirming the presence of sp^2 carbon in Res-CDs (Zhao, Zhou, et al., 2022). The presence of 532.6 and 534.1 eV peaks in the high-resolution O 1 s spectrum (Fig. S1e) indicated the presence of C—O and C═O functional groups (Fan et al., 2021). A high proportion of sp^2-hybridized carbon in the core of CDs and peripheral –OH groups serving as proton donors have been reported to be key structures for imparting CDs with antioxidant activity. Additionally, CDs had a large number of oxygen functional groups on their surface, especially ketone carbon groups, which could promote the production of reactive oxygen species (ROS) and thus exert strong antibacterial effects.

We evaluated the biocompatibility of Res-CDs using MTT assay. As shown in Fig. S2, except for a slight decrease in cell activity in the group with a concentration of 400 μg/mL, there was no significant change in the activity of Caco-2 cells. The cells in the 0–200 μg/mL concentration group showed significant proliferation. This indicates that these Res-CDs have good biocompatibility and the ability to promote cell proliferation.

3.2. Optical and antioxidant properties of res-CDs

Res-CDs exhibited strong absorption properties (Fig. 1a), with peaks at 208 and 275 nm corresponding to n–π* and π–π* transitions of the aromatic structure, respectively (Han et al., 2020). The transmittance spectrum of Res-CDs (Fig. 1b) verified their outstanding UV-shielding capabilities. To examine the FL properties, the Res-CDs solution was excited at 310–380 nm. The optimal excitation and emission wavelengths were 340 and 435 nm, respectively (Fig. 1c and d). In addition, the FL intensities of Res-CDs under different pH conditions were evaluated. As shown in Fig. 2e, the FL intensity of Res-CDs gradually decreased with increasing pH, indicating that Res-CDs had the potential for pH response. The change in intensity may be due to the protonation and deprotonation of various amino and carboxyl groups on the surface of Res-CDs, which disrupts the surface charge and its emissivity

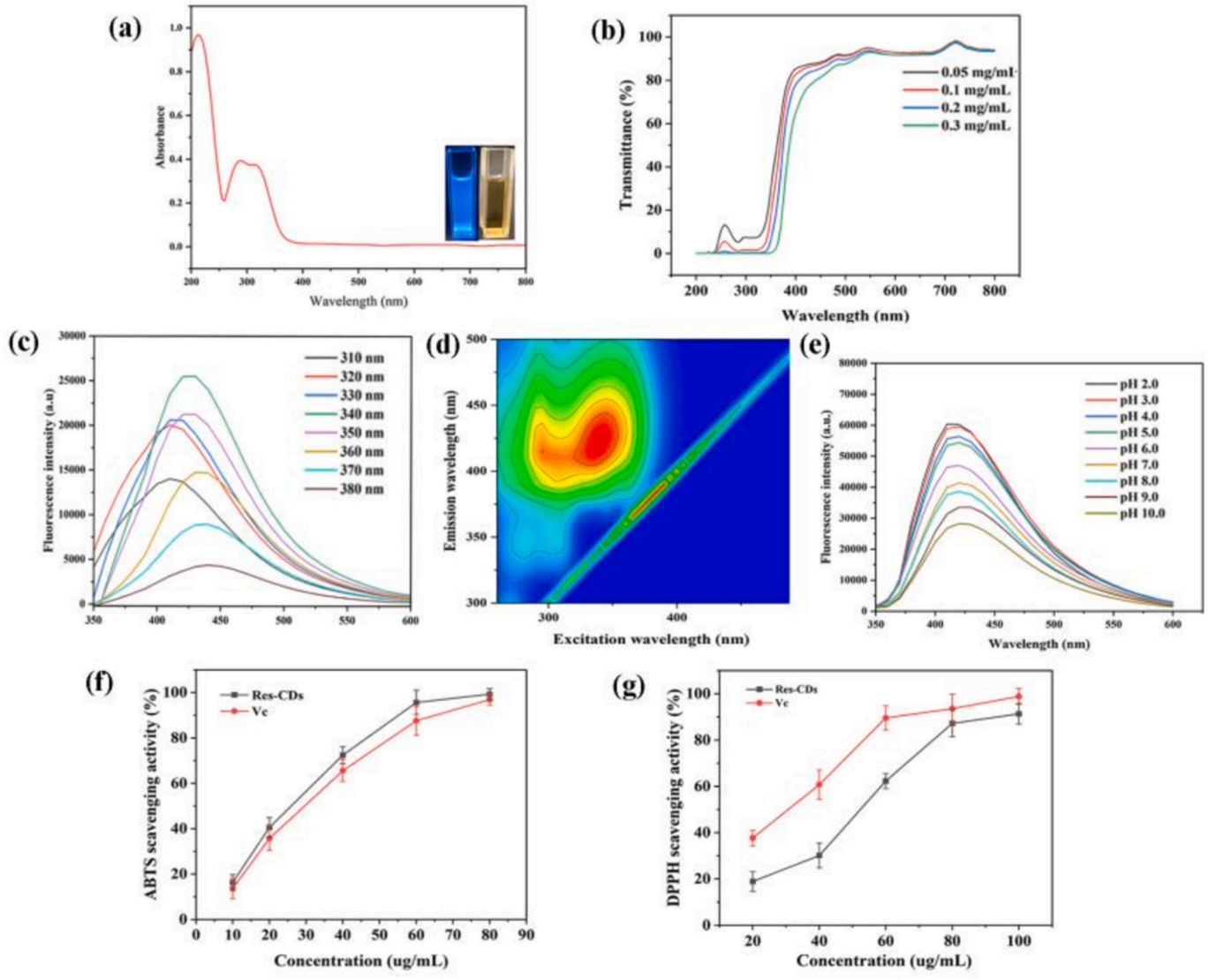

Fig. 1. (a) UV–Vis absorption and (b) transmittance spectra of Res-CDs. (c) FL emission spectra of Res-CDs at different excitation wavelengths. (d) 3D FL spectrum of Res-CDs. (e) Emission spectra of Res-CDs at different pH values. Antioxidant properties of Res-CDs: (f) ABTS and (g) DPPH scavenging activities.

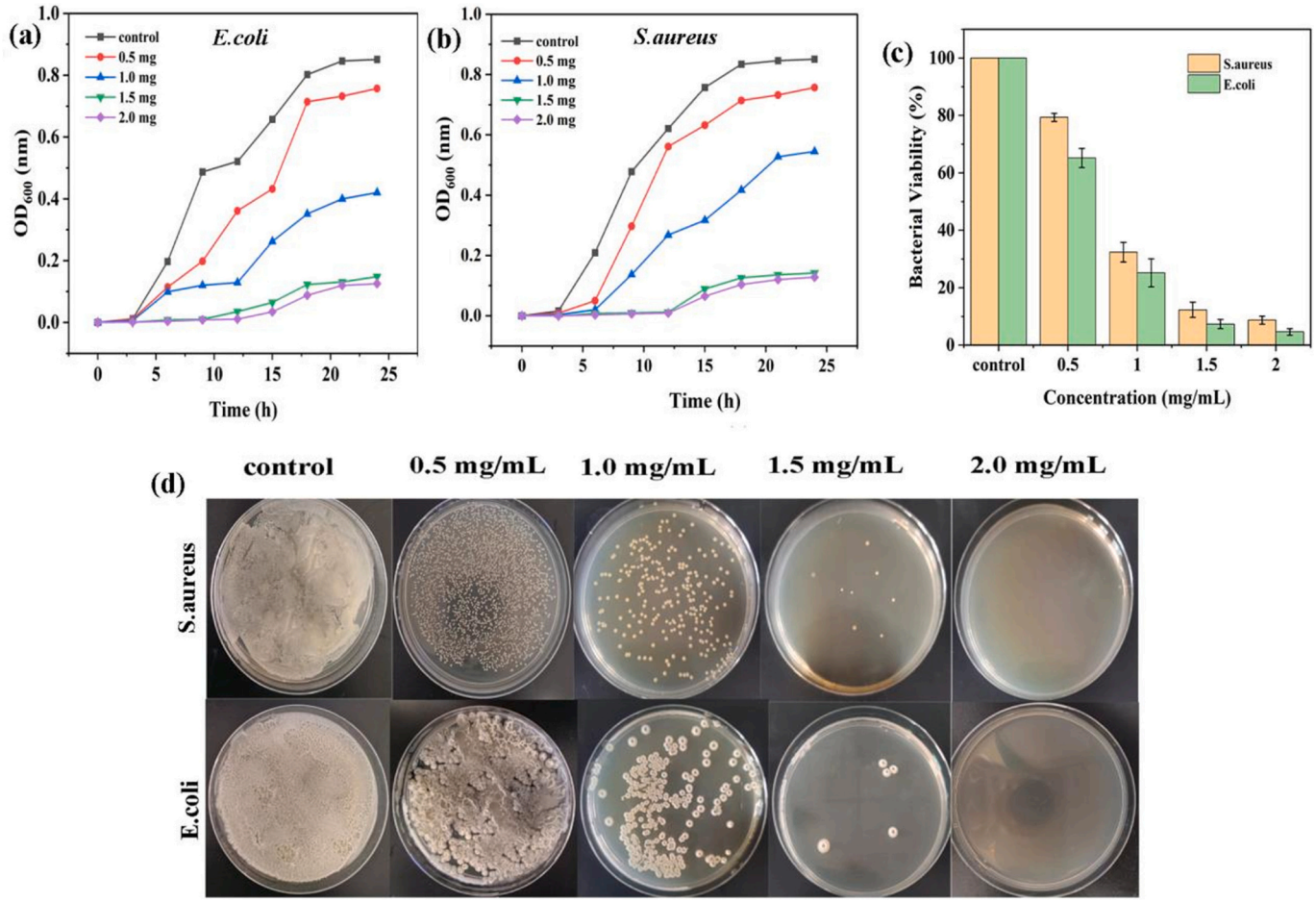

Fig. 2. Bacterial growth curves for varying concentrations of Res-CDs co-incubated with (a) *E. coli* and (b) *S. aureus* for 24 h. (c) Bacterial viability with Res-CDs at different concentration. (d) Colony growth of bacteria treated with Res-CDs at varying concentrations for 24 h.

(Baragau et al., 2021). Importantly, the FL emission maximum did not shift with the change of pH, indicating that the FL properties of Res-CDs were highly stable.

Fig. 1f and g show that the DPPH and ABTS scavenging activities of Res-CDs increased with increasing concentration of Res-CDs. The behavior can primarily be attributed to the aromatic structure of Res-CDs. The structure can provide free-radical scavenging sites, and eliminated free radicals through adcombination and spin delocalization on the conjugated graphene backbone (Luo et al., 2019). Additionally, the abundant numerous hydroxyl groups on the surface of Res-CDs could act as proton donors, transferring free radicals of unpaired electrons to carbon nuclei with C—C backbones (David et al., 2023).

3.3. Antibacterial properties of res-CDs

From Fig. 2a and b, it can be seen that compared with the control group, *E. coli* and *S. aureus* were inhibited, even at the lowest Res-CDs concentration of 0.5 mg/mL. As the concentration of Res CDs increases, the inhibitory effect on bacterial growth gradually strengthens. At a concentration of 1.5 mg/mL, the measured OD value was less than 0.15. Intriguingly, at low concentrations, Res-CDs exhibited superior antibacterial activity against *E.coli* compared to *S.aureus*, possibly due to their different cell wall compositions. The cell wall of Gram-positive bacteria is significantly thicker and more robust compared to that of Gram-negative bacteria. It is composed of 50 to 80 layers of peptidoglycan, providing a substantial protective barrier. In contrast, the cell wall of Gram-negative bacteria contains only 2 to 3 layers of peptidoglycan. Consequently, Res-CDs can destroy the cell walls or penetrate the cells of gram-negative bacteria more rapidly (Fu et al., 2023). We also examined the bacterial viability after treatment with Res-CDs for 24 h (Fig. 2c). With increasing Res-CDs concentration, the survival rate of *E. coli* decreased from 100 % to approximately 5 %, whereas that of *S. aureus* decreased to approximately 8 %, further demonstrating the excellent antibacterial properties of Res-CDs. Additionally, *E. coli and S. aureus* were treated with Res-CDs for 24 h and then standard plate-counting was employed to determine bacterial survival. Fig. 2d shows that the number of colonies decreased with increasing Res-CDs concentration. Numerous colonies were observed at a concentration of 1 mg/mL, but fewer than 10 colonies were present when the concentration of Res-CDs increased to 1.5 mg/mL, suggesting an effective antimicrobial concentration of 1.5 mg/mL. When the concentration of Res-CDs was 2.0 mg/mL, no colonies were present on the plate, indicating that the bacteria were completely inhibited. Res-CDs had a high content of C—O groups, which have been reported to behave as ROS production sites (Castro et al., 2021). It can be inferred that ROS generated at the C—O site of Res-CDs may damage bacterial cell walls, leading to leakage and causing bacterial death.

3.4. Characterization of gelatin/CS/res-CDs films

Leveraging the remarkable antimicrobial properties, pH-responsive and antioxidant capabilities of Res-CDs, they were incorporated into gelatin/CS mixtures to prepare composite films. The physicochemical characteristics of gelatin/CS-based films containing different amounts of Res-CDs were investigated. As shown in Fig. 3a, the color of the films gradually changed to dark yellow as the amount of added Res-CDs

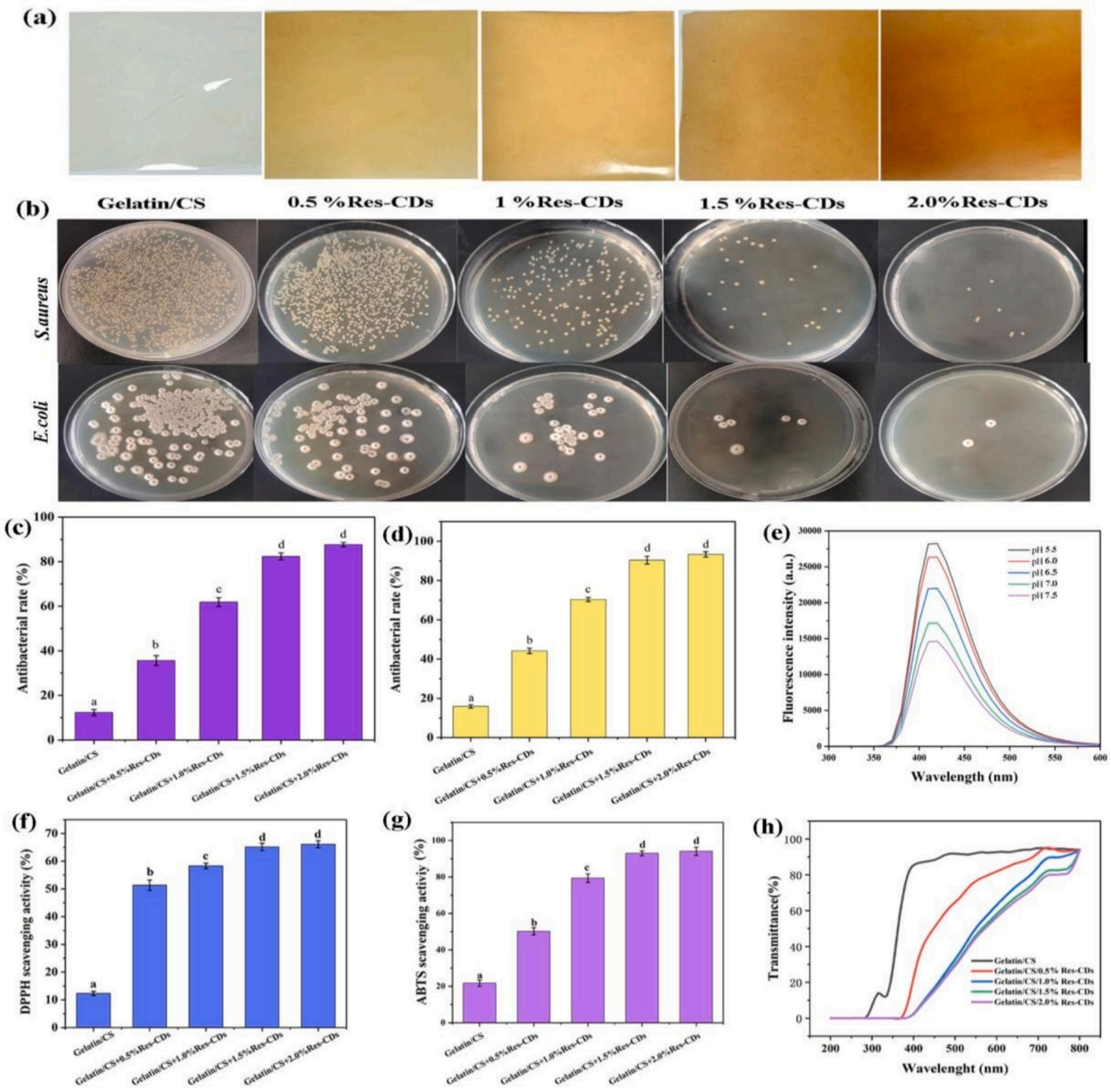

Fig. 3. (a) Photographs of gelatin/CS film and gelatin/CS/Res-CDs films with 0.5 %, 1 %, 1.5 %, and 2 % Res-CDs. (b) Photographs of *E. coli,* and *S. aureus* colonies on agar plates after culture with different concentrations of coating solution and untreated medium. Antimicrobial rates of films against (c) *S. aureus* and (d) *E. coli.* (e) FL intensity of gelatin/CS/Res-CDs films at pH 5.5–7.5. Antioxidant properties of gelatin/CS and gelatin/CS/Res-CDs films: (f) DPPH and (g) ABTS scavenging activities. (h) UV–Vis transmission spectra of gelatin/CS and gelatin/CS/Res-CDs films.

increased, but the flatness of the films did not change significantly. It indicated that the Res-CDs were uniformly dispersed in the gelatin/CS-based films.

3.4.1. Antimicrobial, antioxidant, pH-responsive, and UV-shielding properties of films

The degradation of protein-rich foods releases organic amines, causing a shift in the pH of the surrounding environment. Consequently, pH indicators are prevalent in smart packaging to effectively monitor deterioration. To effectively track this degradation, pH indicators are commonly integrated into smart packaging solutions. Exposure to UV radiation can trigger photochemical reactions in food, resulting in undesirable changes to its color, texture, flavor, and nutritional value. Additionally, oxidative degradation significantly contributes to the loss of food quality. Therefore, it is highly advantageous to incorporate UV-blocking and antioxidant properties into food packaging materials (Katrin & Annika, 2022). However, most reported films only partially block UV radiation. The realization of multifunctional antioxidant, antimicrobial, and pH responsive effects require the incorporation of multiple functional ingredients (Hu et al., 2021).

The antimicrobial capacities of the gelatin/CS-based films against *S. aureus* and *E. coli* were quantitatively evaluated using the colony-counting method (Fig. 3b). The unmodified gelatin/CS film exhibited antimicrobial capacity against *E. coli* and *S. aureus* owing to the

antimicrobial properties of CS (Wrońska et al., 2021). The gelatin/CS/Res-CDs films inherited the bacteriostatic effects of Res-CDs. Thus, as the concentration of Res-CDs in the films increased, the antibacterial activities of the films against *E. coli* and *S. aureus* increased. In addition, the results of the film antibacterial rate showed that compared with the gelatin/CS film, the integration of 1.5 % Res-CDs resulted in increased to 82.36 % and 90.37 % in the antibacterial rates, respectively (Fig. 3c-d). While the antimicrobial capacity of the composite film when the addition of Res-CDs was increased to 2 % was not significantly different from that of 1.5 % ($p < 0.05$).

As shown in Fig. 3e, the composite film (containing 1.5 % Res-CDs) also exhibited pH responsiveness. The FL intensity of the film was strongest at pH 5.5 and gradually decreased as the pH increased. Thus, the gelatin/CS/Res-CDs film has potential as a pH indicator. In addition, to ensure the fluorescence stability of the prepared gelatin/CS/Res-CDs films in natural environments, we measured the fluorescence intensity of films under natural light for 1–9 days. As shown in Fig. S3, the fluorescence of the gelatin/CS/Res-CDs film did not decrease with increasing days, indicating that the film has good fluorescence stability.

Furthermore, the antioxidant capacity of gelatin/CS-based films could be enhanced by adding only a low concentration of Res-CDs as shown in Fig. 3f and g. As the Res-CDs concentration increased, the DPPH and ABTS scavenging activities increased significantly, reaching 64.56 % and 92.27 %, respectively, with 1.5 % Res-CDs. However, upon further increasing the Res-CDs content to 2 %, the antioxidant activity did not change significantly.

The absorbance properties of the films was investigated in the range of 200–800 nm (Fig. 3h). The unmodified gelatin/CS film did not absorb in the UV region (200–400 nm), whereas the films supplemented with only 0.5 % Res-CDs achieved broadband UV absorption. The increased absorbance of the films with Res-CDs could effectively prevent UV rays from entering food. Therefore, the gelatin/CS/Res-CDs composite films had potential for inhibiting lipid oxidation in photosensitized foods. These results indicate that the addition of Res-CDs at a concentration of 1.5 % to gelatin/CS films results in simultaneous antibacterial, pH-responsive, antioxidant, and UV-shielding properties.

3.4.2. *Hydrophobicity, thermal stability, mechanical properties, and cytotoxicity of films*

The WCA indicates the water resistance of a film and is a crucial indicator for assessing the wettability and hydrophobicity of its surfaces, which is predominantly influenced by surface hydrophobicity and morphology of film (Peng et al., 2022). The wettability between a film and the pork influences the formation and in situ adhesion of the film, thereby impacting the effectiveness of preservation. The surface of a biomaterial is considered hydrophilic when the WCA is less than 65°, whereas the surface is considered hydrophobic when the WCA exceeds 90° (Kim et al., 2023; Vogler, 1998). The WCA value of the unmodified

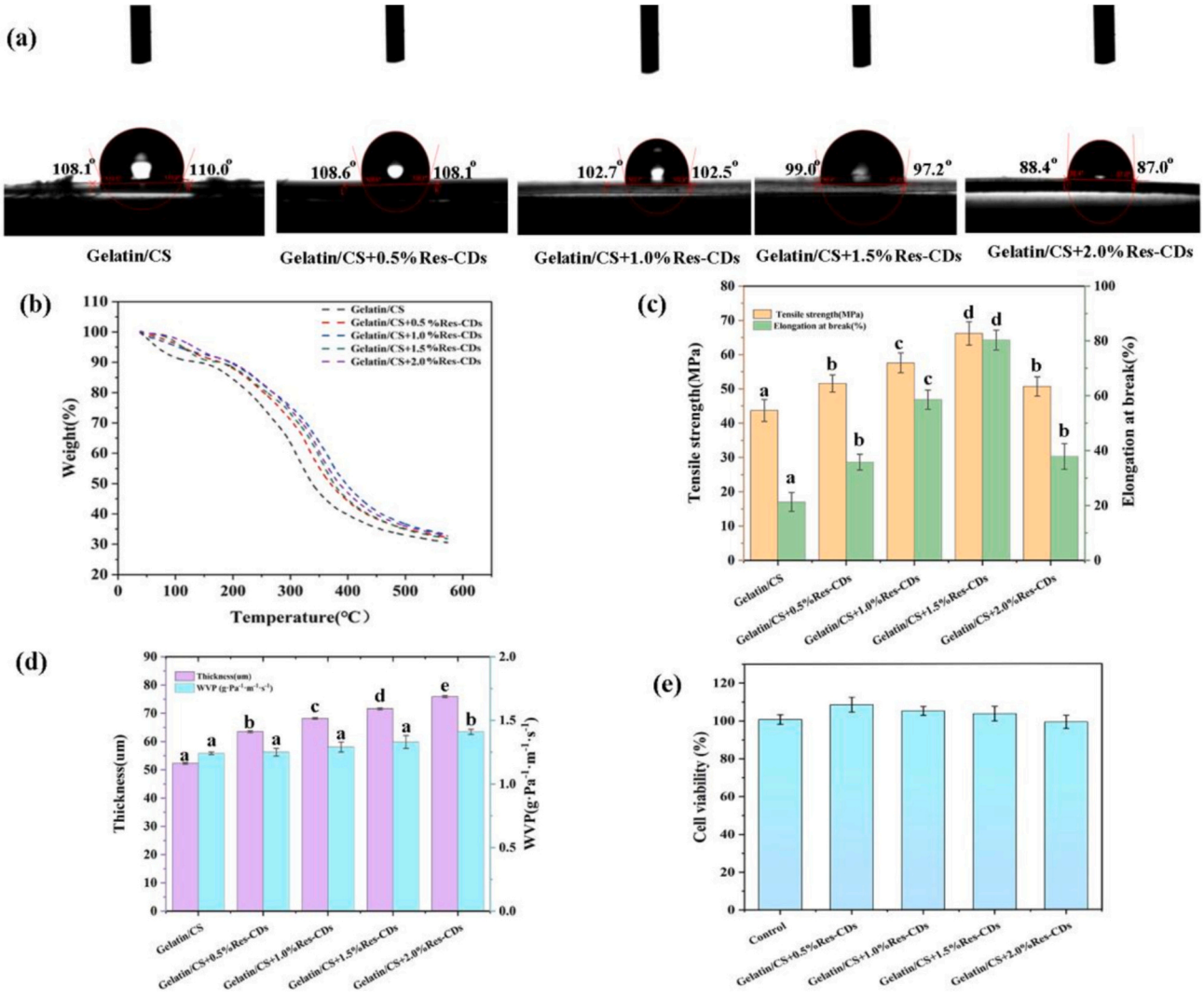

Fig. 4. (a) WCA, (b) TGA thermograms, (c) TS and EB, (d) thickness and WVP, and (e) cell viability of gelatin/CS and gelatin/CS/Res-CDs films.

gelatin/CS film was 108.1° (Fig. 4a), indicating its hydrophobicity. The WCA values of all doped Res-CDs films were lower than those of gelatin/CS film. The increase in hydrophilicity of the composite films was attributed to the presence of hydrophilic groups in Res-CDs (Su et al., 2021). However, the composite films remained hydrophobic, with WCA greater than 65°, which is advantageous for the preparation of food packaging films.

The thermogravimetric analysis (TGA) results show that the gelatin/CS-based films exhibited three thermal degradation stages (Fig. 4b). The initial degradation step (50–130 °C) was attributed to the evaporation of water from the composite films surface, followed by the breaking of intermolecular and intramolecular hydrogen bonds (Zhou et al., 2021). The second degradation step occurred at 130–275 °C owing to the decomposition of glycerol in the films (Yong et al., 2019). The main mass-loss stage occurred at 275–420 °C owing to the decomposition of the high-molecular-weight polymer backbones and Res-CDs (Roy & Rhim, 2022). The TGA in Fig. 4b reveals that Res-CDs impacted the thermal stability of the gelatin/CS films. Owing to their hydrophilic nature, Res-CDs in the film could slow the initial weight loss due to physically adsorbed water molecules. Compared with the unmodified gelatin/CS film, the films with added Res-CDs showed less degradation in the second and third stages and higher thermal stability. The residual carbon content of gelatin/CS and gelatin/CS/Res-CDs films were relatively high (30.84 % and 34.51 %, respectively), mainly because of noncombustible minerals and impurities in the polymer (Bastos et al., 2024). The enhanced thermal stability of the gelatin/CS/Res-CDs films may be ascribed to stronger hydrogen-bonding interactions between Res and the hydroxyl groups of the polymer skeleton.

As shown in Fig. 4c, the TS of the films gradually increased with the increase of Res-CDs addition, and the TS reached the maximum value at 1.5 % of Res-CDs addition. The results showed that the mechanical strength of gelatin/CS-based films could be effectively improved by the moderate addition of Res-CDs, which was mainly due to the fact that Res would interact with the interface between gelatin/CS at a low concentration, and the intermolecular hydrogen bonding was enhanced (Zhou et al., 2024). However, higher addition of Res-CDs decreased the TS of the films, mainly because Res-CDs aggregates disrupt the network structure of gelatin/CS (Freitas et al., 2023). Additionally, the EB of the gelatin/CS-based films increased with the concentration of Res-CDs and reached a maximum at 1.5 % Res-CDs, indicating that the addition of appropriate amounts of Res-CDs simultaneously improved the flexibility of the films.

During food storage and distribution, food quality deteriorates because of the flow of water between the food and the environment. Consequently, films with low WVP have important advantages in preserving food quality (Wang, Liu, et al., 2023). The WVP of the composite film is influenced by the interactions between the filler and polymer matrix. As shown in Fig. 4d, the WVP of the gelatin/CS film was 1.42×10^{-9} g m/m^2 Pa s, and the addition of the optimal amount of Res-CDs (1.5 %) had no significant effect on the WVP vaule of the film. However, the addition of 2 % Res-CDs significantly increased the WVP value of the film, which would affect the food quality and shelf life (Li et al., 2023). Therefore, the experiments chose to add 1.5 % Res-CDs for characterization.

The safety of food packaging materials is critical for ensuring food safety. To determine the biocompatibility of the prepared gelatin/CS-based films, the Caco-2 cells cytotoxicity of the films was investigated. As can be seen in Fig. 4e, with the increase of the concentration of Res-CDs in the films, the cell survival rate did not present significant changes, and all of them were greater than 95 %, which indicated that the prepared composite films had good biocompatibility and could be further applied to food packaging.

Based on the above experimental results, the gelatin/CS-based film with 1.5 % Res-CDs exhibited good antioxidant, antibacterial, UV-resistant, and pH-responsive abilities as well as good thermal stability and mechanical capabilities. Therefore, we selected the film with 1.5 % Res-CDs for subsequent morphological characterization and pork preservation experiments.

3.4.3. Film morphology and structure

The microscopic morphologies of the gelatin/CS films with and without 1.5 % Res-CDs were observed using SEM (Fig. 5a). Some fine particles appeared on the films with added Res-CDs, similar to previously reported results (Bao et al., 2023). This phenomenon was attributed to the upper surface of the film losing moisture faster than the lower surface during drying, leading to the aggregation of Res-CDs (Liu et al., 2024). Nevertheless, the gelatin/CS/Res-CDs film was smooth, and no cracks or voids were observed, indicating that the added Res-CDs were uniformly dispersed in the gelatin/CS matrix and that a stable, uniform network structure was formed. The corresponding AFM images (Fig. 5b) show that the composite film containing 1.5 % Res-CDs was rougher than the gelatin/CS film. In addition, the height profile of the film is shown in Fig. S4. As shown in the figure, the height profile of the film with 1.5 % Res-CDs added was higher than that of the gelatin/CS film. This observation was consistent with the SEM results, which was mainly due to the aggregation of Res-CDs. In addition, it can be seen from the figure that the gelatin/CS/Res-CDs film was darker than the gelatin/CS film because Res-CDs were dark brown in color.

As shown in Fig. 5c, the gelatin/CS and gelatin/CS/Res-CDs films exhibited similar FTIR spectra. The addition of Res-CDs did not cause significant changes in the functional groups on the films, indicating that the Res-CDs were completely mixed with the gelatin/CS matrix to form compatible films. The broad peak at 3378 cm^{-1} was mainly due to hydrogen bonding between Res-CDs, CS, and glycerol. The peaks around 1689 and 1528 cm^{-1} corresponded to amide I band vibrations owing to C—O stretching and amide II vibrations owing to N—H bending, respectively (Roy et al., 2020). The peak at 1453 cm^{-1} was attributed to C—N stretching vibrations. The peak at 1248 cm^{-1} corresponded to the amide III band, representing in-plane vibrations of C—N and N—H groups in bound amides (Qi et al., 2017). In addition, the peak at 1035 cm^{-1} was attributed to C—O stretching vibrations. The FTIR spectrum of the gelatin/CS/Res-CDs film showed stronger peak intensities, indicating an increase in amine, hydroxyl, and hydrogen-bonding interactions in the composite film. These results suggest that Res-CDs were successfully incorporated into the gelatin/CS matrix and that hydrogen bonds formed between gelatin/CS and Res-CDs (Chen et al., 2019).

3.5. Packaging test with pork

To evaluate the practical applicability of the developed gelatin/CS/Res-CDs film, a packaging test was performed using pork. Fig. S5 shows the changed in appearance of packaged pork after 6 days of storage at 20 °C. From the figure, it can be seen that the pork packed with gelatin/CS/Res-CDs film slowly darkened the color of the meat with the increase of storage time, but there was no appearance of bacterial colonies on the surface of the pork. In contrast, the color of pork packed with gelatin/CS film darkened significantly with the extension of storage time, and colonies appeared on the surface of pork at 4 days of storage, and the area of colonies increased with the extension of time. Unpackaged pork undergoes significant color changes with prolonged storage time, accompanied by dehydration. On the third day of storage, bacterial colonies appeared on the surface of the pork. This indicated that the gelatin/CS/Res-CDs film had good antibacterial property and could effectively prolong the shelf life of pork.

As Fig. 6a shows that the pH of pork rose as storage time extended, which was attributed to the breakdown of pork proteins and the buildup of amines. Compared with the control group (unpackaged and packaged with gelatin/CS), the pH of pork packaged with gelatin/CS/Res-CDs film increased slowly, indicating that gelatin/CS/Res-CDs film can effectively slow down the breakdown of pork protein. As the gelatin/CS/Res-CDs film exhibited pH-responsive FL property, the FL intensity of the composite films were recorded during storage. The results show that the

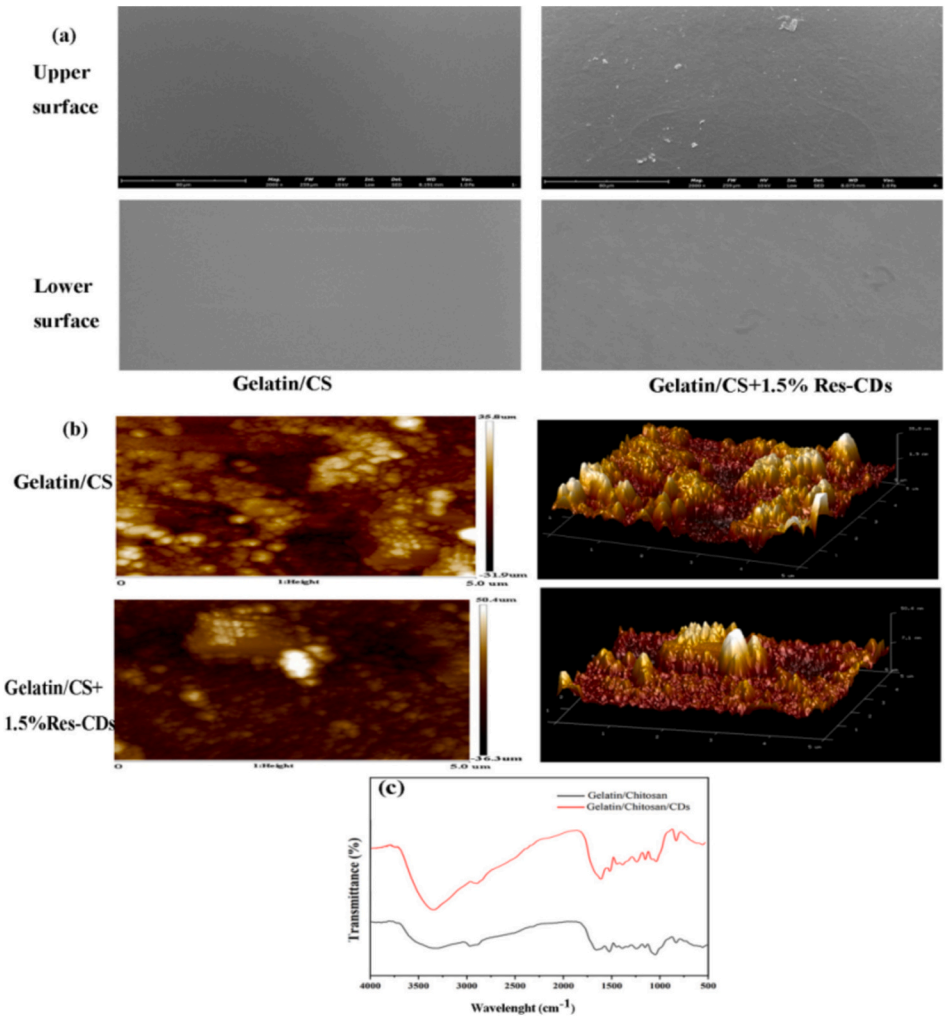

Fig. 5. (a) SEM images, (b) AFM images, and (c) FTIR spectra of gelatin/CS and gelatin/CS/Res-CDs films.

FL intensity of the gelatin/CS/Res-CDs films decreased progressively (Fig. 6b). In addition, Fig. S6 similarly shows that the prepared gelatin/CS/Res films were highly sensitive to pH, and the FL intensity of the films decreases rapidly as the number of storage days increases. This indicated that gelatin/CS/Res-CDs films had good pH optical sensitivity and could be used for monitoring the freshness of pork.

Protein breakdown in pork was determined by measuring TVB-N. As shown in Fig. 6c, the TVB-N value gradually increased with storage time. Among all groups, the control group showed the highest TVB-N value, exceeding the limit value (15 mg/100 g) specified in the National Standard GB 2707–2016 of the People's Republic of China in less than 3 days. In contrast, the TVB-N values of the gelatin/CS and gelatin/CS/Res-CDs films exceeded the limit on the 4th and 6th day, respectively. This trend suggested that gelatin/CS/Res-CDs films can delay TVB-N production, confirming their suitability for hindering the breakdown of proteins in pork (Mousavi et al., 2021).

Additionally, changes in the TVC of the pork samples were recorded (Fig. 6d). GB/T 9959.2–2008 standard stipulates that the TVC of edible pork should not exceed 6.0 lg CFU/g. The study measured that the TVC value of fresh pork was 3.15 lg CFU/g, and the TVC value of unpacked pork increased rapidly to 7.41 lg CFU/g on the 3rd day, which indicated that the pork had already deteriorated at this time and was not edible. However, the TVC of pork packaged with the gelatin/CS and gelatin/CS/Res-CDs films slowly increased, reaching 5.98 and 6.02 lg CFU/g on the 3rd and 5th days, respectively, which indicated that the composite films inhibited the increase in the microbial population of pork. Because both CS and Res-CDs effectively inhibit microbial growth and have good antibacterial properties, the gelatin/CS/Res-CDs film was able to reduce the TVC.

Fig. 6e shows the variation of the a value of pork during the storage process. The gradual decrease in this value was attributed to the oxidation of unstable oxygenated myoglobin ($MbFeIIO_2$) and deoxyhemoglobin (MbFeII) to brown methemoglobin (MbFeBIII) (Wang et al., 2024). Compared with the control group, the pork packaged with the gelatin/CS/Res-CDs film had a higher a value. This behavior was attributed to the antioxidant activities of CS and Res-CDs, which endowed the composite film with oxygen barrier properties. In addition, complexes formed by myoglobin with compounds such as H_2S and H_2O_2 produced by microorganisms may lead to discoloration. Therefore, the antimicrobial activities of CS and Res-CDs could also contribute to the relatively high a value of pork packaged with the composite film.

The weight of pork decreased continuously during storage (Fig. 6f), indicating that the nutritional loss of pork (Zhou et al., 2024). However, the weight loss with the gelatin/CS/Res-CDs group was consistently lower than that with the gelatin/CS group or control. Protection from UV light is a key factor in controlling nutrient loss. As the Res-CDs were shown to have UV-resistant properties, integrating Res-CDs into the composite film may hinder nutrient degradation by blocking a certain amount of UV light, thus reducing weight loss (Gui et al., 2024).

TBA is an important indicator of lipid oxidation. The initial TBA value of pork was 0.015 mg MDA/kg as shown in Fig. 6 g. On the sixth day of storage, the TBV value of unpacked pork was 0.594 mg MDA/kg,

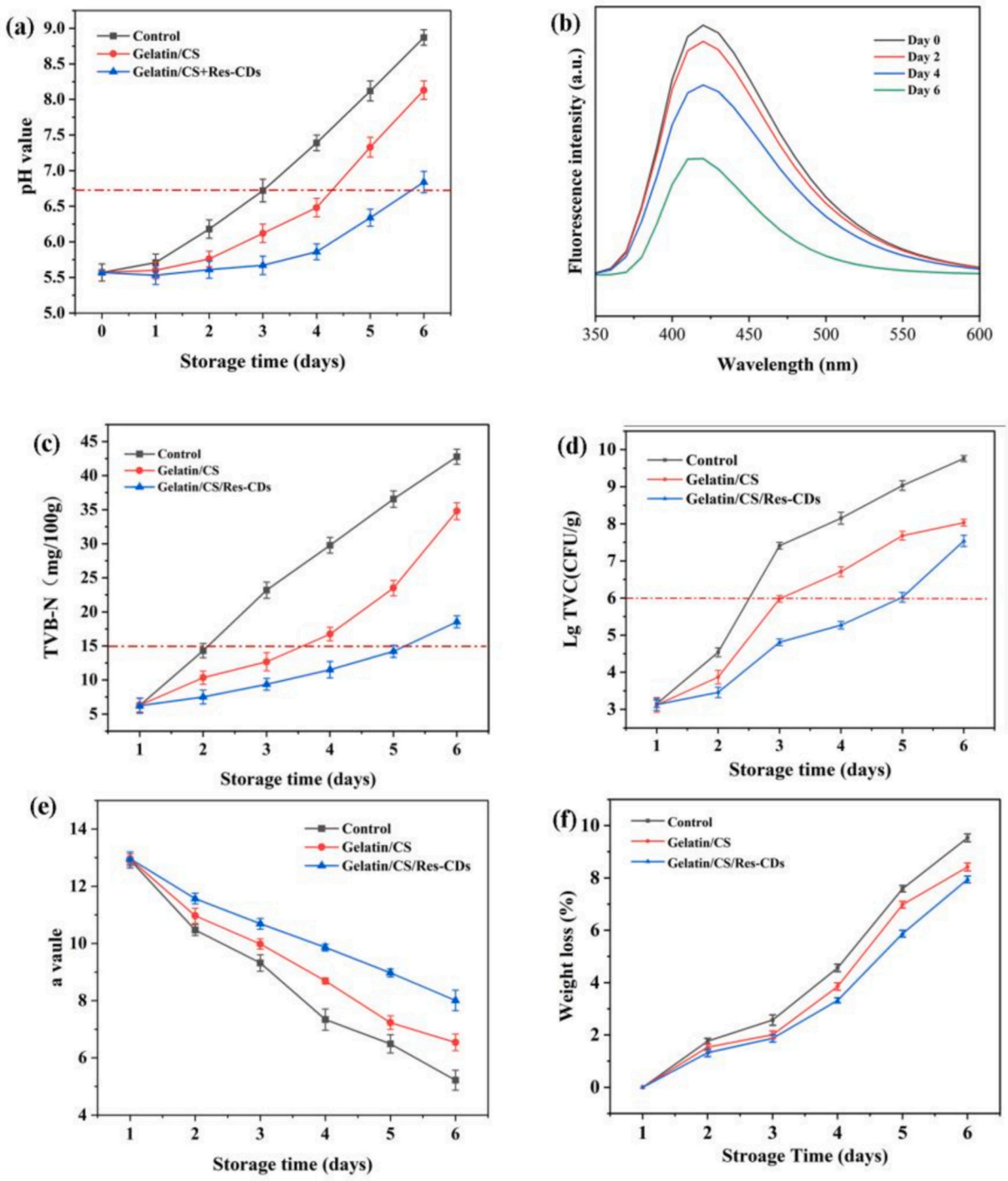

Fig. 6. (a) pH values of pork during storage. (b) FL spectra of gelatin/CS/Res-CDs film used to wrap pork (excitation wavelength = 340 nm). (c) TVB-N, (d) TVC, (e) a values, (f) weight loss, and (g) TBA values of pork during storage unwrapped (control) and wrapped in gelatin/CS or gelatin/CS/Res-CDs films.

indicating that severe oxidization of pork had occurred. In contrast, the TBA value of the gelatin/CS/Res-CDs film group increased slowly during storage, and the TBA value on the 6th day of storage was 0.013 mg MDA/kg, which was significantly lower than that of the control and gelatin/CS groups. This was mainly due to the strong free radical scavenging ability of Res-CDs, and their addition into gelatin/CS-based films could effectively reduce the degree of pork oxidation.

4. Conclusion

In this study, Res-CDs with antibacterial, antioxidant, pH-responsive, and UV-shielding properties were successfully prepared using a one-pot hydrothermal method. The corresponding bionanocomposite film based on gelatin/CS/Res-CDs inherited the functional characteristics of Res-CDs, was noncytotoxic, and exhibited excellent hydrophilicity and mechanical properties. When applied as packaging, the gelatin/CS/Res-CDs film had the best protective effect on pork quality, extending the shelf life by 3 days. In addition, the gelatin/CS/Res-CDs film maintained lower TBC and pH values in pork, and the changes in TVB-N and TBA levels indicated a decrease in the degree of lipid oxidation in pork during storage. Furthermore, owing to the pH-sensitive nature of the FL properties of Res-CDs under UV (λ = 340 nm) irradiation, the gelatin/CS/

Res-CDs film could act as an indicator of pork freshness.

CRediT authorship contribution statement

Tianxin Fu: Writing – original draft, Investigation, Funding acquisition, Data curation, Conceptualization. **Yuchao Feng:** Resources, Methodology, Conceptualization. **Shu Zhang:** Methodology. **Yanan Sheng:** Conceptualization. **Changyuan Wang:** Writing – review & editing, Supervision, Resources, Project administration.

Declaration of competing interest

The authors declare that they have no known competing financial interests or personal relationships that could have appeared to influence the work reported in this paper.

Acknowledgments

This work was supported by the Rapid identification of bacteria and their antimicrobial properties based on fluorescent carbon dots (ZRCQC202308), Preparation of antimicrobial carbon dots and their application in food packaging (XYB202320).

Appendix A. Supplementary data

Supplementary data to this article can be found online at https://doi.org/10.1016/j.fochx.2025.102182.

Data availability

Data will be made available on request.

References

Bao, J. J., Hu, Y. Y., Farag, M. A., Huan, W. W., Wu, J. S., Yang, D. P., & Song, L. L. (2023). Carbon dots, cellulose nanofiber, and essential oil nanoemulsion from Torreya grandis aril added to fish scale gelatin film for tomato preservation. *International Journal of Biological Macromolecules, 245(1), Article 125482*. https://doi.org/10.1016/j.ijbiomac.2023.125482

Baragau, I.-A., Lu, Z., Power, N. P., Morgan, D. J., Bowen, J., Diaz, P., & Kellici, S. (2021). Continuous hydrothermal flow synthesis of S-functionalised carbon quantum dots for enhanced oil recovery. *Chemical Engineering Journal, 405, Article 126631*. https://doi.org/10.1016/j.cej.2020.126631

Bastos, B. M., da Silva, P. P., da Rocha, S. F., Bertolo, J., de Oliveira Arias, J. L., Michelon, M., & de Almeida Pinto, L. A. (2024). Preparation of films based on reticulated fish gelatin containing garlic essential oil. *Food Research International, 188, Article 114496*. https://doi.org/10.1016/j.foodres.2024.114496

Bogireddy, N. K. R., Lara, J., Fragoso, F. R., & Agarwal, V. (2020). One-step hydrothermal preparation of highly stable N doped oxidized carbon dots for toxic organic pollutants sensing and bioimaging. *Chemical Engineering Journal, 401*, 1385–8947. https://doi.org/10.1016/j.cej.2020.126097

Calva-Estrada, S. J., Jimenez-Fernandez, M., & Lugo-Cervantes, E. (2019). Protein-based films: Advances in the development of biomaterials applicable to food packaging. *Food Engineering Reviews, 11*(2), 78–92. https://doi.org/10.1007/s12393-019-09189-w

Castro, B., Citterico, M., Kimura, S., Stevens, D. M., Wrzaczek, M., & Coaker, G. (2021). Stress-induced reactive oxygen species compartmentalization, perception and signalling. *Nature Plants, 7*, 403–412. https://doi.org/10.1038/s41477-021-00887-0

Chen, H. G., Lan, X. N., Guan, X., Luo, R. W., Zhang, Q., Ren, H. F., … Tang, J. (2024). Comparative study on the effects of chitosan, carrageenan, and sodium alginate on the film-forming properties of fish skin gelatin. *LWT - Food Science and Technology, 199*, Article 116111. https://doi.org/10.1016/j.lwt.2024.116111

Chen, Q. J., Zhou, L. L., Zou, J. Q., & Gao, X. (2019). The preparation and characterization of nanocomposite film reinforced by modified cellulose nanocrystals. *International Journal of Biological Macromolecules, 132*, 1155–1162. https://doi.org/10.1016/j.ijbiomac.2019.04.063

Chen, X., Liang, L., & Han, C. (2020). Borate suppresses the scavenging activity of gallic acid and plant polyphenol extracts on DPPH radical: A potential interference to DPPH assay. *LWT, 131, Article 109769*. https://doi.org/10.1016/j.lwt.2020.109769

Cheng, H. Y., Zhao, Y. F., Wang, Y., Hou, Y. X., Zhang, R., Zong, M. R., … Li, B. (2023). The potential of novel synthesized carbon dots derived resveratrol using one-pot green method in accelerating in vivo wound healing. *International Journal of Nanomedicine, 18*, 6813–6828. https://doi.org/10.1016/j.lwt.2020.109769

David, T., Nemoto, J., Bian, K. J., Kao, S. H., & West, J. (2023). Radical ligand transfer: A general strategy for radical functionalization. *Beilstein Journal of Organic Chemistry, 19*, 1225–1233. https://doi.org/10.3762/bjoc.19.90

Ezati, P., Khan, A., Priyadarshi, R., Bhattacharya, T., Tammina, S. K., & Rhim, J. W. (2023). Biopolymer-based UV protection functional films for food packaging, *food hydrocolloids. Article, 142*, Article 108771. https://doi.org/10.1016/j.foodhyd.2023.108771

Fan, K., Zhang, M., Guo, C., & Devahastin, S. (2021). Laser-induced microporous modified atmosphere packaging and chitosan carbon-dot coating as a novel combined preservation method for fresh-cut cucumber. *Food and Bioprocess Technology, 14*, 968–983. https://doi.org/10.1007/s11947-021-02617-y

Fang, Z. X., Zhao, Y. Y., Warner, R. D., & Johnson, S. K. (2017). Active and intelligent packaging in meat industry. *Trends in Food Science & Technology, 61*, 60–71. https://doi.org/10.1016/j.tifs.2017.01.002

Freitas, P. A. V., González-Martínez, C., & Chiralt, A. (2023). Active poly (lactic acid) films with rice straw aqueous extracts for meat preservation purposes. *Food and Bioprocess Technology, 16*, 2635–2650. https://doi.org/10.1007/s11947-023-03081-6

Fu, B. F., Liu, Q. L., Liu, M. H., Chen, X. F., Lin, H. T., Zheng, Z. Q., … Yang, D. P. (2022). Carbon dots enhanced gelatin/chitosan bio-nanocomposite packaging film for perishable foods. *Chinese Chemical Letters, 33*, 4577–4582. https://doi.org/10.1016/j.cclet.2022.03.048

Fu, T. X., Wan, Y., Jin, F. R., Liu, B. W., Wang, J. D., Yin, X. Y., … Feng, Z. B. (2023). *Efficient imaging based on P - and N-codoped carbon dots for tracking division and viability assessment of lactic acid bacteria, colloids and surfaces B: Biointerfaces. 223*, Article 113155. https://doi.org/10.1016/j.colsurfb.2023.113155

Gui, N. N., Zhang, X. X., Yang, C., Ran, R. M., Yang, C. K., Zeng, X. L., & Li, G. Y. (2024). A high-strength collagen-based antimicrobial film grafted with ε-polylysine fabrication by riboflavin-mediated ultraviolet irradiation for pork preservation. *Food Chemistry, 461, Article 140889*. https://doi.org/10.1016/j.foodchem.2024.140889

Guo, B. Y., Liu, G., Ye, W. H., Xu, Z. Q., Li, W., Zhuang, Z. L., … Dong, H. W. (2024). Multifunctional carbon dots reinforced gelatin-based coating film for strawberry preservation. *Food Hydrocolloids, 147, Article 109327*. https://doi.org/10.1016/j.foodhyd.2023.109327

Haghighi, H., Biard, S., Bigi, F., Leo, R. D., Bedin, E., Pfeifer, F., … Pulvirenti, A. (2019). Comprehensive characterization of active chitosan-gelatin blend films enriched with different essential oils. *Food Hydrocolloids, 95*, 33–42. https://doi.org/10.1016/j.foodhyd.2019.04.019

Han, Y., Yang, W., Luo, X., He, X., Zhao, H., Tang, W. Y. T., & Li, Z. (2020). Carbon dots based ratiometric fluorescent sensing platform for food safety. *Critical Reviews in Food Science and Nutrition, 62*(1), 244–260. https://doi.org/10.1080/10408398.2020.1814197

Hu, Z., Wang, H. L., Li, L. L., Wang, Q., Jiang, S. W., Chen, M. M., … JiangS, T. (2021). pH-responsive antibacterial film based polyvinyl alcohol/poly (acrylic acid) incorporated with aminoethyl-phloretin and application to pork preservation. *Food Research International, 147, Article 110532*. https://doi.org/10.1016/j.foodres.2021.110532

Jia, F., Yan, W. J., Yuan, X. L., Dai, R. T., & Li, X. M. (2019). Modified atmosphere packaging of eggs: Effects on the functional properties of albumen. *Food Packaging and Shelf Life, 22, Article 100377*. https://doi.org/10.1016/j.fpsl.2019.100377

Katrin, M. B., & Annika, O. (2022). In R. Bhat, & F. Foods (Eds.), *Chapter 21-innovations in food packaging-sustainability challenges and future scenarios* (pp. 375–392). https://doi.org/10.1016/B978-0-323-91001-9.00039-6

Kim, Y. H., Kim, H., Yoon, K. S., & Rhim, J. (2023). Cellulose nanofiber/deacetylated quaternary chitosan composite packaging film for growth inhibition of listeria monocytogenes in raw salmon. *Food Packaging and Shelf Life, 35, Article 101040*. https://doi.org/10.1016/j.fpsl.2023.101040

Kurian, M., & Paul, A. (2021). Recent trends in the use of green sources for carbon dot synthesis–a short review. *Carbon Trends, 3, Article 100032*. https://doi.org/10.1016/j.cartre.2021.100032. Retrieved from https://www.sciencedirect.com/science/article/pii/S2667056921000092.

Li, H. G., Ning, X., Solveig, H., & Andreas, D. (2019). Resveratrol and vascular function. *International Journal of Molecular Sciences, 20*(9), 2155. https://doi.org/10.3390/ijms20092155

Li, J. X., Bao, Y. B., Li, Z. Y., Cui, H. J., Jiang, Q., Hou, C. L., … Li, B. (2023). Dual-function β-cyclodextrin/starch-based intelligent film with reversible responsiveness and sustained bacteriostat-releasing for food preservation and monitoring. *International Journal of Biological Macromolecules, 253(5), Article 127168*. https://doi.org/10.1016/j.ijbiomac.2023.127168

Liu, J. P., Zhang, Y. Q., Liu, W. W., Gao, B. Y., & Yu, L. L. (2020). A novel Zein-based composite nanoparticles for improving bioaccessibility and anti-inflammatory activity of resveratrol. *Foods, 10*(11), 2773. https://doi.org/10.3390/foods10112773

Liu, Z. B., Cui, M., Weng, R. E. H. C., Li, H. B., Hati, S., Hu, L. B., & Mo, H. Z. (2024). Incorporation of carbon dots into polyvinyl alcohol/corn starch based film and its application on shiitake mushroom preservation. *International Journal of Biological Macromolecules, 280(3), Article 135998*. https://doi.org/10.1016/j.ijbiomac.2024.135998

Luo, H., Papaioannou, K., Salvadori, E., Roessler, M., Ploenes, G., van Eck, E., … Yang, Y. (2019). Manipulating the optical properties of carbon dots by fine-tuning their structural features. *ChemSusChem, 12*(19), 4432–4441. https://doi.org/10.1002/cssc.201901795

Md Shimul, B., Raihan, C., Mst Asma, A., Md Arman, A., Meher, A., Md Showkot, A., … Muhammad, T. (2024). A mechanistic insight into the anticancer potentials of resveratrol: Current perspectives. *Phytotherapy Research, 38*, 3877–3898. https://doi.org/10.1002/ptr.8239

Min, S., Ezati, P., & Rhim, J. W. (2022). Gelatin-based packaging material incorporated with potato skins carbon dots as functional filler. *Industrial Crops and Products, 181, Article 114820*. https://doi.org/10.1016/j.indcrop.2022.114820

Mohammadi, R., Mohammadifar, M. A., Rouhi, M., Kariminejad, M., Mortazavian, A. M., Sadeghi, E., & Hasanvand, S. (2018). Physico-mechanical and structural properties of eggshell membrane gelatin- chitosan blend edible films. *International Journal of Biological Macromolecules, 107*, 406–412. https://doi.org/10.1016/j.ijbiomac.2017.09.003

Mousavi, S. N., Daneshvar, H., Seyed Dorraji, M. S., Ghasempour, Z., Panahi-Azar, V., & Ehsani, A. (2021). Starch/alginate/ cu-g-C3N4 nanocomposite film for food packaging. *Materials Chemistry and Physics, 267, Article 124583*. https://doi.org/10.1016/j.matchemphys.2021.124583

Oh, W. Y., & Shahidi, F. (2017). Lipophilization of resveratrol and effects on antioxidant activities. *Journal of Agricultural and Food Chemistry, 65*(39), 8617–8625. https://doi.org/10.1021/acs.jafc.7b03129

Peng, L., Dai, H. J., Wang, H. X., Zhu, H. K., Ma, L., Yu, Y., … Zhang, Y. Z. (2022). Effect of different dehydration methods on the properties of gelatin films. *Food Chemistry, 374*, Article 131814. https://doi.org/10.1016/j.foodchem.2021.131814

Qi, M., Zhou, Y., Huang, Y., Zhu, L., Xu, X., Ren, Z., & Bai, J. (2017). Interface-induced terahertz persistent photoconductance in rGO-gelatin flexible films. *Nanoscale, 9*, 637–646. https://doi.org/10.1039/c6nr06573b

Rekha, R. K., Jijo, T. K., Siji, K. M., Sandeep, S. S. J., & Laly, A. (2021). Pothan preparation of pH sensitive film based on starch/carbon nano dots incorporating anthocyanin for monitoring spoilage of pork. *Food Control, 126*, Article 108039. https://doi.org/10.1016/j.foodcont.2021.108039

Ren, L. L., Yan, X. X., Zhou, J., Tong, J., & Su, X. G. (2017). Influence of chitosan concentration on mechanical and barrier properties of corn starch/chitosan films. *International Journal of Biological Macromolecules, 105*(3), 1636–1643. https://doi.org/10.1016/j.ijbiomac.2017.02.008

Riahi, Z., Rhim, J. W., Bagheri, R., Pircheraghi, C., & Lotfali, E. (2022). Carboxymethyl cellulose-based functional film integrated with chitosan-based carbon quantum dots for active food packaging applications. *Progress in Organic Coatings, 166, Article 106794*. https://doi.org/10.1016/j.porgcoat.2022.106794

Roy, S., & Rhim, J. W. (2022). Genipin-crosslinked gelatin/chitosan-based functional films incorporated with rosemary essential oil and quercetin. *Materials, 15, Article 3769*. https://doi.org/10.3390/ma15113769

Roy, S., van Hai, L., Kim, H. C., Zhai, L., & Kim, J. (2020). Preparation and characterization of synthetic melanin-like nanoparticles reinforced chitosan nanocomposite films. *Carbohydrate Polymers, 231*, Article 115729. https://doi.org/10.1016/J. CARBPOL.2019.115729

Settier-Ramirez, L., López-Carballo, G., Hernandez-Muñoz, P., Tinitana-Bayas, R., Gavara, G., & Sanjuán, N. (2022). Assessing the environmental consequences of shelf life extension: Conventional versus active packaging for pastry cream. *Journal of Cleaner Production, 333, Article 130159*. https://doi.org/10.1016/j.jclepro.2021.130159

Su, L., Huang, J., Li, H., Pan, Y., Zhu, B., Zhao, Y., & Liu, H. (2021). Chitosan-riboflavin composite film based on photodynamic inactivation technology for antibacterial food packaging. *International Journal of Biological Macromolecules, 172*, 231–240. https://doi.org/10.1016/j.ijbiomac.2021.01.056

Sul, Y. J., Ezati, P., & Rhim, J. W. (2023). Preparation of chitosan/gelatin-based functional films integrated with carbon dots from banana peel for active packaging application. *International Journal of Biological Macromolecules, 246, Article 125600*. https://doi.org/10.1016/j.ijbiomac.2023.125600

Tripathi, S., Kumar, L., Deshmukh, R. K., & Gaikwad, K. K. (2024). Ultraviolet blocking films for food packaging applications. *Food and Bioprocess Technology, 17*, 1563–1582. https://doi.org/10.1007/s11947-023-03221-y

Uranga, J., Puertas, A. I., Etxabide, A., Dueñas, M. T., Guerrero, P., & de la Caba, K. (2019). Citric acid-incorporated fish gelatin/chitosan composite films. *Food Hydrocolloids, 86*, 95–103. https://doi.org/10.1016/j.foodhyd.2018.02.018

Vogler, E. A. (1998). Structure and reactivity of water at biomaterial surfaces. *Advances in Colloid and Interface Science, 74*, 69–117.

Wang, F. Q., Xu, Z. P., Chen, L., Qiao, A. Y., Hu, Y. Y., Fan, X. J., … Feng, X. C. (2024). Super absorbent resilience antibacterial aerogel with curcumin for fresh pork preservation. *Food Control, 159, Article 110289*. https://doi.org/10.1016/j.foodcont.2024.110289

Wang, Y., Li, L., & Hu, J. (2023). Development of biobased multifunctional films incorporated with essential oils@polydopamine nanocapsules for food preservation applications. *International Journal of Biological Macromolecules, 253*(5), Article 127161. https://doi.org/10.1016/j.ijbiomac.2023.127161

Wang, Y. X., Liu, K., Zhang, M., Xu, T., Du, H. S., Pang, B., & Si, C. L. (2023). Sustainable polysaccharide-based materials for intelligent packaging. *Carbohydrate Polymers, 313, Article 120851*. https://doi.org/10.1016/j.carbpol.2023.120851

Wrońska, N., Katir, N., Miłowska, K., Hammi, N., Nowak, M., Kędzierska, M., … Lisowska, K. (2021). Antimicrobial effect of chitosan films on food spoilage bacteria. *International Journal of Molecular Sciences, 22*(11), 5839. https://doi.org/10.3390/ijms22115839

Yildirim, S., Röcker, B., Pettersen, M. K., Nilsen-Nygaard, J., Ayhan, Z., Rutkaite, R., … ComaActive, V. (2018). Active packaging applications for food. *Comprehensive Reviews in Food Science and Food Safety, 17*, 165–199. https://doi.org/10.1111/1541-4337.12322

Yong, H., Wang, X., Bai, R., Miao, Z., Zhang, X., & Liu, J. (2019). Development of antioxidant and intelligent pH-sensing packaging films by incorporating purple-fleshed sweet potato extract into chitosan matrix. *Food Hydrocolloids, 90*, 216–224. https://doi.org/10.1016/j.foodhyd.2018.12.015

Zhao, L. L., Zhang, M., MujumdarBenu, A. S., Adhikari, B., & Wang, H. X. (2022). Preparation of a novel carbon dot/polyvinyl alcohol composite film and its application in food preservation. *ACS Applied Materials & Interfaces, 14*(33), 37528–37539. https://doi.org/10.1021/acsami.2c10869

Zhao, Y. L., Zhou, S. Y., Xia, X. D., Tan, M. Q., Lv, Y. N., Cheng, Y., … Wang, H. S. (2022). High-performance carboxymethyl cellulose-based hydrogel film for food packaging and preservation system. *International Journal of Biological Macromolecules, 223*, 1126–1137. https://doi.org/10.1016/j.ijbiomac.2022.11.102

Zhou, T. X., Wang, H. L., Han, Q., Song, Z. P., Yu, D. H., Li, G. D., … Chen, X. (2024). Fabrication and characterization of an alginate-based film incorporated with cinnamaldehyde for fruit preservation. *International Journal of Biological Macromolecules, 274, Article 133398*. https://doi.org/10.1016/j.ijbiomac.2024.133398

Zhou, W., He, Y. X., Liu, F., Liao, L. K., Huang, X. B., Li, R. Y., & Li, J. H. (2021). Carboxymethyl chitosan-pullulan edible films enriched with galangal essential oil: Characterization and application in mango preservation. *Carbohydrate Polymers, 256*. https://doi.org/10.1016/j.carbpol.2020.117579

Glossary

ABTS: 2,2′-azino-bis(3-ethylbenzothiazoline-6-sulfonic acid)
AFM: atomic force microscopy
A_b: background absorbance
A_c: control absorbance
A_s: sample absorbance
A_1: absorbance of control sample
A_2: absorbance of Res-CDs sample
CD: carbon dot
CS: chitosan
DPPH: 2,2-diphenyl-1-picrylhydrazyl
FL: fluorescence
FTIR: Fourier transform infrared
N_1: number of bacterial colonies in the film-treated group
N_2: number of bacterial colonies in the control group
OD: optical density
OD600–1: optical density at 600 nm after coculturing Res-CDs with bacteria
OD600–2: optical density at 600 nm of bacterial solution without Res-CDs
Res: resveratrol
ROS: reactive oxygen species
SEM: scanning electron microscopy
TBA: thiobarbituric acid
TEM: transmission electron microscopy
TGA: thermogravimetric analysis
TVB-N: total volatile basic nitrogen
TVC: total viable bacteria count
UV: ultraviolet
UV–Vis: ultraviolet–visible
WCA: water contact angle
WVP: water vapor permeability
XPS: X-ray photoelectron spectroscopy
XRD: X-ray diffraction